Joint Stress Estimation and Remaining Useful Life Prediction for Collaborative Robots to Support Predictive Maintenance

Emil Stubbe Kolvig-Raun, Mikkel Baun Kjærgaard, and Ralph Brorsen

***Abstract*—Anticipating the maintenance needs of lightweight robotic manipulators at precise future instances represents a significant challenge within the automation domain. This letter introduces an innovative and comprehensive method to estimate the severity of stress imposed on a robot joint at any given time. Additionally, we present a knowledge-based predictive model aimed at approximating the End of Life (EoL) for a robotic joint, enabling the prediction of its Remaining Useful Life (RUL) with respect to the designated load case. This predictive model is rooted in a baseline derived from empirical data covering the entire Universal Robots (UR) e-series and is trained using synthetic data. Subsequently, it undergoes evaluation with a real-world dataset and is further validated in a case study. The model demonstrates a high level of accuracy, with worst-case performance reaching 90.3% as the lower limit.**

***Index Terms*—Collaborative robots in manufacturing, formal methods in robotics and automation, industrial automation, robot manipulators, predictive maintenance.**

I. Introduction

MAINTENANCE has emerged as a critical cornerstone in robotics and industrial manufacturing, where even the slightest operational disruption can lead to significant production loss. Comprehensive maintenance strategies can improve production quality and enhance the efficiency and effectiveness of operational processes, thereby contributing to increased profitability and output [1]. In the current industry, maintenance strategies predominantly revolve around Time-Based and Condition-based maintenance paradigms, often called preventive maintenance [2].

According to research, maintenance operations account for 15% to 60% of total expenses [3] and underscores the imperative for more refined maintenance strategies. This need has fueled the adoption of Predictive Maintenance (PdM) in robotics, which relies on technologies and methods to anticipate equipment's Remaining Useful Life (RUL) [4]. Accurate information about when equipment is expected to fail empowers operators to make more knowledgeable decisions when scheduling future maintenance.

In the domain of lightweight robotic manipulators, also commonly known as collaborative robots (cobots), current research predominantly concentrates on forecasting the degradation of specific components within the robot [5], [6], [7]. However, focusing solely on individual parts can result in misleading assessments, as estimating the lifespan of select components does not necessarily align with the overall remaining lifespan of the entire robot.

Addressing this gap, this letter presents a novel method that estimates the stress impeded on a robot joint, denoted as α, by taking outset in measurements derived from the overarching robot control system, thereby naturally considering the load case, environment, and the intrinsic constellation of acting components. This stress estimate is further employed in a knowledge-based model to predict the RUL in number of program cycles, denoted as δ. A conceptual overview of the contribution is presented in Fig. 1.

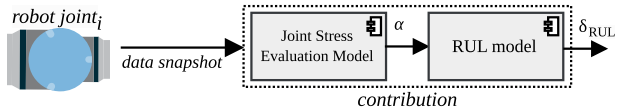

Fig. 1. Contribution concept overview, where α denotes joint stress, and δ a number of cycles.

The work conducted in this letter is based on data collected from the entire range of robots within the UR e-series, including 408 cobots and 1424 joints. We test our model on a dataset of 54 failed joints and further validate it in a case study using two UR16e cobots. The model performs with a worst-case accuracy of 90.3%.

The case study results are compared to a baseline using the industry-standard gearbox lifetime equation [9], [10]. With this equation, we also aim to demonstrate the concept of a misleading assessment as it only focuses on a particular component.

II. Related Work

Predicting the RUL of components is a well-recognized challenge across a diverse array of fields. While mechanical and electrical engineering domains have witnessed extensive research endeavors to construct and refine methods for modeling and predicting fault occurrences and wear patterns in specific

Manuscript received 23 October 2023; accepted 4 February 2024. Date of publication 21 February 2024; date of current version 4 March 2024. This letter was recommended for publication by Associate Editor W. Guo and Editor C.-B. Yan upon evaluation of the reviewers' comments. This work was supported by the Innovation Fund Denmark for the project DIREC under Grant 9142-00001B. *(Corresponding author: Emil Stubbe Kolvig-Raun.)*

Emil Stubbe Kolvig-Raun is with SDU Software Engineering, University of Southern Denmark, 5000 Odense, Denmark, and also with Universal Robots, 5260 Odense, Denmark (e-mail: eskr@mmmi.sdu.dk, eskr@universal-robots.com).

Mikkel Baun Kjærgaard is with SDU Software Engineering, University of Southern Denmark, 5000 Odense, Denmark (e-mail: mbkj@mmmi.sdu.dk).

Ralph Brorsen is with Universal Robots, 5260 Odense, Denmark (e-mail: rbr@universal-robots.com).

Digital Object Identifier 10.1109/LRA.2024.3368296

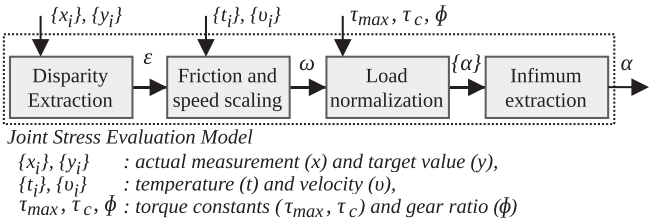

Fig. 2. Method overview for the joint stress evaluation equation model (α). Note that ϵ and ω are outputs from the preceding components.

components, this concept has yet to mature in robotics. Notable methods originating from electrical engineering encompass the utilization of stochastic modeling and survival functions, primarily applied to predict battery resistance alterations for lifespan prognostics [11], [12]. Researchers have also explored image-based strategies to classify worn factory equipment [13]. Similarly, works like [14] have harnessed anomaly detection models to monitor many different machines, unveiling insights into their health status based on temporal interactions.

In the context of robotics and condition monitoring, research has predominantly relied on vibration measurements, employing various methods, ranging from deep autoencoders to short-time Fast Fourier transforms, to anticipate the lifespan of gear bearings [5], [6], [7]. Vibration measurements have also been used in simulation to model joint shear displacement in relation to fatique [8]. These techniques pinpoint damage points by recognizing when vibration amplitudes surpass a predetermined threshold. Nonetheless, these approaches exhibit limitations concerning precision, adaptability to diverse bearing types, and the scope of prognosis, as they are primarily oriented toward assessing specific components. Additionally, researchers have sought to develop models for monitoring the health of robot tools [6], [15], without addressing manipulator components. In alignment with the nature of these contributions, particular noteworthy works have explored specific trends in the hysteresis curve of joint gears to gain insights into wear patterns [16]. Other contributions, exemplified by works such as [17], [18], have directed their attention to estimating execution times by assessing program functions.

However, rather than zooming in on particular mechanical and/or electrical components, our method embraces a holistic viewpoint by measuring how well the entire joint operates according to the control system's expectations, rooting the assessment of RUL in a broader range of components.

III. A Method to Evaluate Joint Stress

The term *stress* has been previously used in studies for structural optimization of robots [19]. We define *stress*, denoted as α, as any duress that impacts the health of the joint. Stress impacts the operational lifetime [20], and joints in poor condition experience heightened susceptibility to stress. Fig. 2 presents the proposed method to estimate the stress imposed on a joint. Furthermore, the figure presents the input required to use the method in practical applications.

A. Method Foundation

Our mathematical approach builds on the basis that during execution, robot systems operate with outset in target values, i.e.,

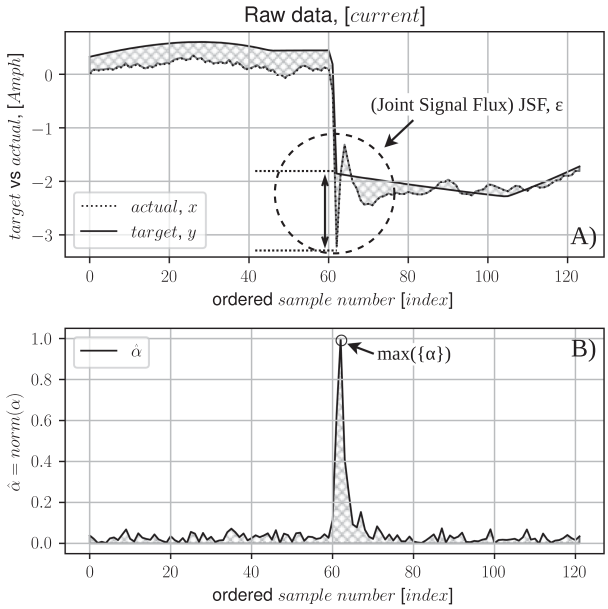

Fig. 3. (a) Visualizes measurements on electrical current from a worn UR5e robot shoulder joint; target versus actual, in ampere. It can be seen how the actual current overshoots during changes in rotational speed and direction. (b) Visualizes the normalized computed α sequence.

values that are theoretically assumed [21]. For example, when the robot moves, the system computes the required electrical currents (amperes). Concurrently, real-time measurements are conducted and utilized as feedback to continuously and accurately adjust the target values. Due to disparities between the real-world physical state and the mathematical model, discrepancies commonly emerge between the target values and the actual measurements.

We denote these discrepancies as Joint Signal Fluxes (JSFs), depicted in Fig. 3(a), where the signal (actual current) fluctuates upon sudden incrementation of the joint's rotational speed and direction. Furthermore, declare that attributed to wear *these JSFs increase over time of use*, caused by the dynamic nature of the physical state of the robot joint (later detailed in Section III-C).

Merely quantifying the magnitude of the JSF, in isolation from a reference point, does not inherently provide insights into the state of the joint. First, by identifying the magnitude and after that factoring in three primary challenges, can the severity of the discrepancy be compared one-to-one across various robot joints:

i) Robot tasks: The programmable nature of robots enable the execution of custom procedures, consequently yielding disparate signal values.
ii) Environment: Changes in temperature and variations in load impact the materials of a robot joint, leading to differing friction levels.
iii) Varying models: Robot manipulators span a spectrum of sizes possessing distinct joint dimensions, requiring different operational resources, i.e., different joints can withstand varying forces.

B. Mathematical Formulation

The formulation in (1) shows that the computations are conducted on a time series obtained by recording the robot joint

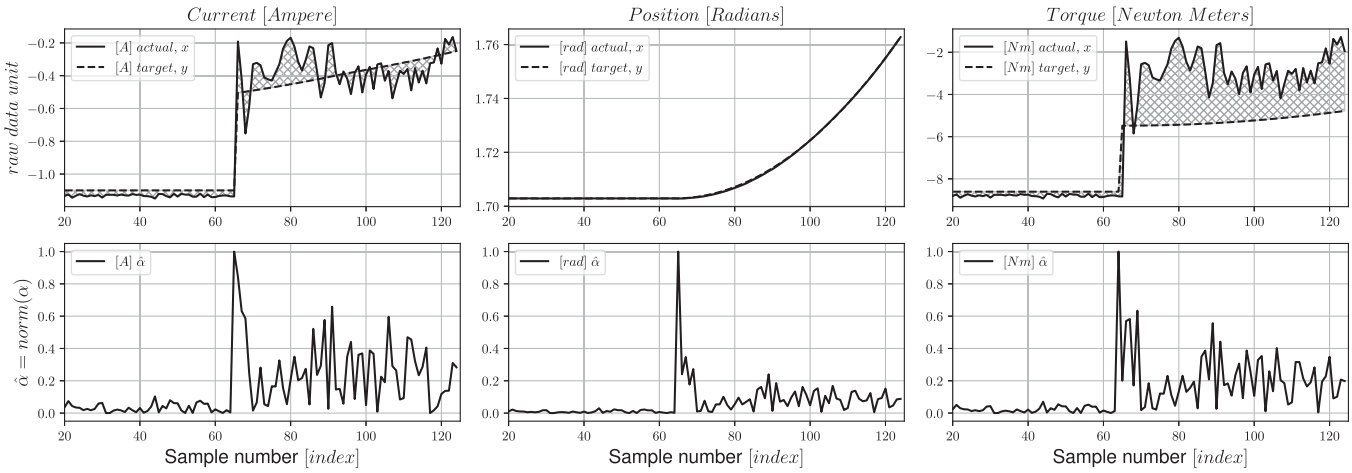

Fig. 4. Example of α computed relative to different robot state variables, including electrical current (ampere), joint position (radians), and torque (Newton-Meters). The data in this example originates from a UR10 robot shoulder joint. The results are similar for all other e-series joints.

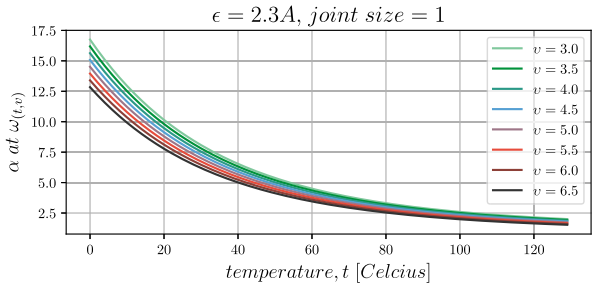

Fig. 5. Illustrates how α is scaled according to $w_{(t,\omega)}$ at $\epsilon = 2.3$ A.

in operation, where i refers to a particular datapoint within the sequence of measurements, i from $0 \rightarrow \mathbb{Z}^+$. With the sequence as outset the infimum, i.e., the greatest value accounting for erroneous outliers, can be extracted to indicate the worst-case JSF (depicted in Fig. 3(b)). The infimum is, among others, used for later RUL calculations, further described in Section V.

$$\max_{i \in [0, \mathbb{Z}^+]} \{\alpha(\epsilon, \omega, \phi, \tau_k, \tau_{\max})_i\} \tag{1}$$

The computation of α is conducted relative to ϵ, which denotes the absolute JSF between the physical state and the overarching model, described in (2).

In the following examples of this letter, we have taken an outset in the electrical currents, such that x_i is the actual measurement, and y_i is the robot system's calculated target value. However, as indicated in Fig. 4, variable robot state variables with high correlation provide similar results, meaning that the infimum originating from any of these computations *could potentially* be used instead.

$$\epsilon_{(x_i, y_i)} = |x_i - y_i| \tag{2}$$

To evaluate the severity of ϵ relative to the joint composition, the result is scaled according to the weighting function ω, described in (3) and depicted in Fig. 5.

$$\omega_{(v,t)} = (|\upsilon_{\max}| - |v|) * (e^{c_0} * c_1 + e^{c_2 * t} * c_3)^2 \tag{3}$$

where the right-hand side of the equation is a combination of two terms; the left-hand term depends on the absolute velocity, υ (radians per second), and a constant defining the absolute maximal velocity, $\upsilon_{\max}$. The right-hand term is formulated based on the temperature-dependent friction coefficient model [20], [22] and must resemble how changes in friction are computed in the robot control system. The robot manufacturer establishes the model, often expressed as a decaying exponential function. It depends on a set of constants, $c_{(0,\ldots,3)}$, obtained during joint calibration, and the temperature, t. Consequent to this weighting function, ϵ is penalized such that high-velocity rotations leading to a specific error level are considered less detrimental than low-velocity rotations yielding the same error magnitude, e.g., with an increase in structural temperatures, there is an expected reduction in joint rigidity, which aligns with the anticipation of increased error magnitudes and, therefore, inversely penalized.

The joint stress estimation method , as shown in (4), unifies all elements in the computational process and yields a positive numerical value.

$$\alpha_i = \left| \left[\frac{\epsilon \omega \phi \tau_k}{\tau_{\max}} \right]_{[i]} - \left[\frac{\epsilon \omega \phi \tau_k}{\tau_{\max}} \right]_{[i-1]} \right|, \quad \forall i \in \{1, \ldots, (n-1)\} \tag{4}$$

where n represents the length of the sequence of measurements, indexed from 0 to $n-1$ and i starts at 1.

Following the joint type, an associated resistance to force exists, essentially denoting the maximum load threshold the joint can sustain prior to breakdown. The closeness of the current load to this maximum indicates the current level of stress the joint is experiencing. The concept is factored in by incorporating the maximum torque, $\tau_{\max}$, the gear ratio (number of teeth), ϕ, and the torque constant, τ_k. According to $\tau = I * \tau_k * \phi$ [22], this constant describes the electrical input and torque correlation.

Finally, the computation subtracts the preceding value result to calculate the absolute Rate of Change (ROC), introducing a filter that efficiently illuminates abnormal changes in the error magnitude.

C. Temporal Evolution of α

Attributing any health-related meaning to α necessitates the establishment of a reference. This was achieved by acquiring

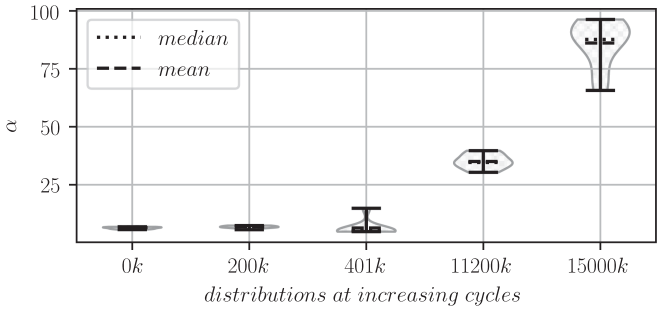

Fig. 6. α's equated from accelerated life tests (with aim to wear the gears) across an increasing number of cycles. Each distribution contains 10 α-infimums.

empirical data from accelerated life tests designed to wear the gears conducted on the various joint sizes in the UR e-series.

Testing protocol: Each of the joints (sizes) was separately mounted on a pedestal, equipped with a mass to serve as the mechanical load and inertia, and configured to oscillate clock-wise and counter-clock-wise driven at highly accelerated velocity. Each rotation constitutes a single program cycle. The electrical current (target and actual) was recorded at the 0, 200, 400 thousandth, 11.2, and 15 millionth cycle at 500 Hertz. Ten infimum (to account for outliers) JSF values were extracted from each recording along with their prevailing rows. From this data, the α values were calculated according to the method presented in Section III-B.

Fig. 6 presents the α values distribution across the logged cycles, highlighting the temporal evolution. Note that the x-axis is non-linear.

The results indicate a rising trend, thereby showing an increase in the discrepancy between the physical state and the expectations of the robot control system along with continuous use over time, attributed to progressive joint deterioration.

Because the temporal evolution is derived from electrical currents, its applicability is linked to amperage consumption. Nonetheless, this scope is by no means limited, given that any motion necessitates power and, intuitively, directly contributes to wear.

IV. α's Coherency With Robot Joint Condition

To demonstrate the applicability of α as an indicator of the joints condition, we evaluate whether the magnitude of α can be used to distinguish healthy from faulty robot joints.

We acquired two real-world datasets extracted from log files generated during protective stops. A protective stop is triggered by the safety system when the robot does not behave according to expectations or enters a singularity, i.e., impossible move configurations. Up to four log files can be stored at once, and each contains the most recent entries documented by the RTDE interface [23], typically a time series of 30 seconds recorded with a frequency of 500 Hertz. For each joint, the infimum JSF value and its prevailing row were extracted from the protective stop log file to calculate α. Note that both datasets encapsulate all available joint sizes within the e-series.

Dataset 1: Denoted as $H\sim$, comprises 1370 data rows from log files of different *healthy joints* (those operating within specs) across 395 robots. The healthy robots were subjected to pick-and-place operations, shaking, and sweeps at maximal velocity while carrying their maximal payload.

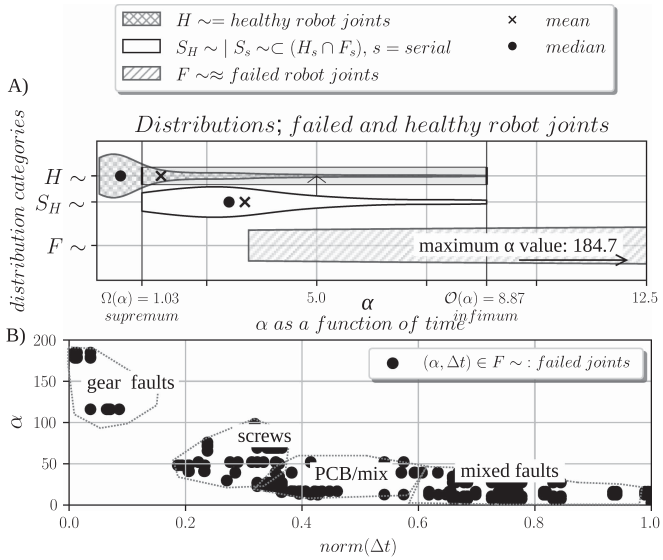

Fig. 7. A) Violin plot highlighting local spreading. S_H is a subset of H such that S_s comprise the intersection of serial numbers between H, F. B) Shows the relationship between α, normalized operation time, and types of faults.

Dataset 2: Denoted as $F\sim$, comprises 203 data rows from log files of *faulty joints*, from 54 different joints across 13 robots. Breakdowns linked to mechanical wear due to continued operation have been included exclusively. Therefore, $F\sim$ does *not* contain breakdowns related to direct damage or errors in the software system.

Fig. 7(a) visually depicts both datasets and their distribution. $H\sim$ with a mean of 1.45 and a median of 0.53. $F\sim$ with 24.78 and 11.61, respectively. In Fig. 6, the mean of the distribution at 0 cycles approximates $\lceil 0.4$. However, it is based on fewer values than $H\sim$. Log files generated from protective stops are not guaranteed to represent the load case accurately, as these do not necessarily encompass the entire program cycle. Therefore, we anticipate the true population mean of $H\sim$ to be lower than the result in Fig. 7(a). Nevertheless, this does not apply to $F\sim$ because protective stops indicate faults.

The S_H distribution, also seen in Fig. 7(a), was created from $H\sim$ and $F\sim$. S_H contains the α values in $H\sim$ that originates from the same joints as seen in $F\sim$. As described in the figure legend, the filtering was done by comparing serial numbers, s. From the minimum value of S_H, the supremum $\Omega(\alpha)$ is denoted at 1.03 to indicate that robot joints displaying α values above the supremum exhibit signs of early degradation. Similarly, the maximal value of S_H denotes the infimum $\mathcal{O}(\alpha)$ at 8.87.

The wide distribution of $F\sim$ illustrates that robot joints do not consistently fail at the same α threshold. This is supported by Fig. 7(b), which describes the relationship between α, normalized operation time, Δt, and observed types of faults. Note that *PCB* refers to Printed Circuit Board and electrical faults, while *screws* are structural.

The results indicate that specific components exhibit an elevated risk of failure, depending on the magnitude of stress imposed and the joint's total operation time.

V. A Model To Predict Remaining Useful Life

Historically, robot state variables such as torque and a comprehensive understanding of differential equations have

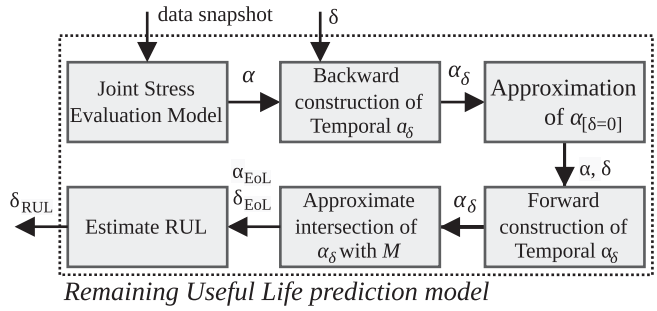

Fig. 8. Method overview of the RUL model. Note that δ denotes a cycle count and α_δ models the temporal evolution of α. M is a set of functions.

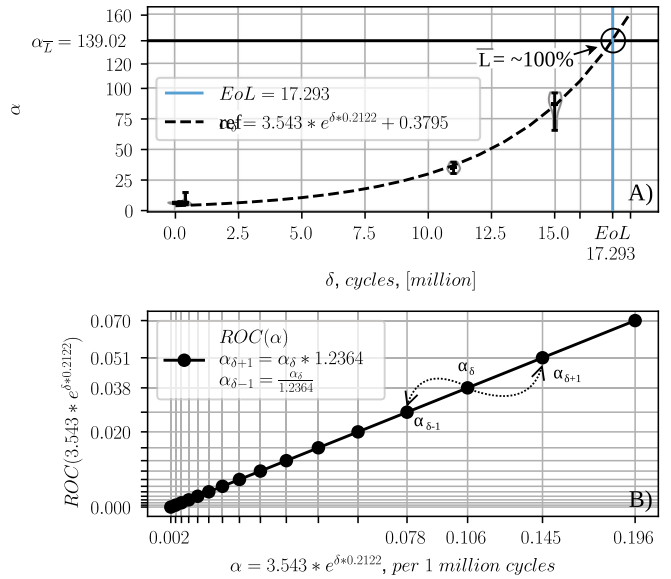

Fig. 9. Calculation of a temporal reference for predicting RUL. A) shows α as a function of δ (cycles in millions), and B) shows how the ROC scales linearly proportional to the increase of α according to the incrementation of 1 per million cycles, δ.

been used for condition monitoring and the isolation of temporal trends [24], [25]. In our study, we utilize α to establish a knowledge-based model that estimates a robot joint's RUL through approximation of the End of Life (EoL).

The facilitation involves establishing a temporal reference model from the accelerated life tests (described in Section III-C) and using it as the outset to generalize across a broader range of robot joint breakdowns and runtime durations by training the model, denoted as M, on a larger *synthetic* dataset. The model's method is highlighted in Fig. 8, incorporating the equations on joint stress from Section III-B.

A. Modelling The Temporal Evolution of α

Based on the dataset acquired from the experiment on temporal evolution in Section III-C, we characterize the behavior with the exponential function seen in (5), where α is expressed as a function of cycles, δ. The function is denoted as temporal α_δ. Note that the choice to facilitate the model with an exponential was based on *best fit*.

$$\alpha_\delta \approx \alpha_{[\delta=0]} * e^{\delta * \lambda} + \overline{x}_{[H(\alpha \leq \Omega(\alpha))]} \tag{5}$$

where λ and $\alpha_{[\delta=0]}$ are both rate parameters, λ is a constant dependent on the temporal evolution and $\alpha_{[\delta=0]}$ is calculated according to the method presented in Section III-B. $\overline{x}$ is the mean of $H\sim$ before the supremum, $\Omega(\alpha)$, assuming an average outset for α_δ at $\delta = 0$.

The final approximation, ref, is numerically presented in (6) and visually depicted in Fig. 9(a). We use ref as the reference model to describe temporal α_δ of the experiment.

$$ref \approx \lceil 3.453 \rceil * e^{\delta * \lceil 0.2122 \rceil} + \lceil 0.3795 \rceil \tag{6}$$

This can also be used as a reference in practical applications.

B. Approximating The EoL for the Reference Model

With (5) to describe temporal α_δ of the accelerated life tests designed to wear the joints gears, ref, we calculate the expected EoL based on the industry-standard gearbox lifetime equation to identify the point of failure [9], [10]. The equation ascertains the time at which 10% of the gears are projected to fail and serves as the formula commonly employed during gear specification tests. It is shown in (7).

$$\overline{L} = \frac{L10}{L_n} * 100, \quad L10 = L_n \frac{\nu_n}{\nu_{avg}} \left(\frac{\tau_n}{\tau_{avg}} \right)^3 \tag{7}$$

L_n signifies the nominal lifetime of the gear in hours. N represents the number of samples in the load case. ν_n is the rated speed in Rotations Per Minute (RPM), while ν_{avg} is the average speed. τ_n is the rated torque, and τ_{avg} the average torque. Note that rated loads depend on the particular gear model and that the actual torque, as opposed to the target torque, is required as input for the equation. This distinction arises because the latter is a calculated value considerably influenced by the robot control system.

$\overline{L}$ denotes the percentical representation. To estimate the expected EoL, we perform the calculation of $\overline{L}$ based on the distribution at the 15 millionth cycle, equating to $\approx 60\%$, and extrapolate α at $\overline{L} = 100\%$, denoted as $\alpha_{\overline{L}}$.

As visualized in Fig. 9(a), given Eqs. (6) and (7), the accelerated life test, thus the temporal reference model, obtains $\alpha_{\overline{L}} = 139.02$ and EoL$= 17.293$ million cycles.

C. Back -and Forward Construction of Temporal α_δ

Based on the temporal reference model, ref, depicted in Fig. 9(a), we establish a method facilitating the estimation of $\alpha_{\delta-1}$ (backward) and $\alpha_{\delta+1}$ (forward) with $\alpha_{[\delta=n]}$ as the input. This method approximates temporal α_δ, given a specific cycle count, n. The concept is illustrated in Fig. 9(b). Without a cycle count, $\alpha_{[\delta=n]}$ is assumed as $\alpha_{[\delta=0]}$ and only forward construction is completed.

Fig. 9(b) graphs the ROC; the derivative of the exponential function, as a function of α proportional to a continuous increment of one million cycles (δ). The exponential growth of α evens out, and the result becomes a linear function, as seen in (8).

$$\alpha_{\delta-1} = \frac{\alpha_{[\delta=n]}}{1.2364}, \quad \alpha_{\delta+1} = \alpha_{[\delta=n]} * 1.2364 \tag{8}$$

where n is the current cycle count. As a result, when provided with a robot joint and a load case, we can predict the anticipated

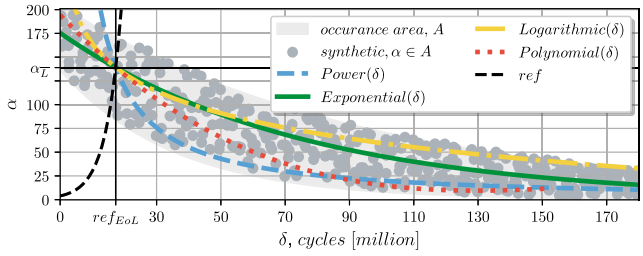

Fig. 10. Visualizes the fitting of each approximation function to the temporal reference, ref, and the $synthetic$ dataset.

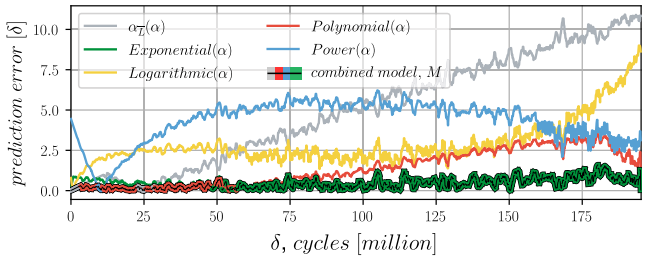

Fig. 11. Visualizes the creation of M, the sequence of approximation functions with the lowest error.

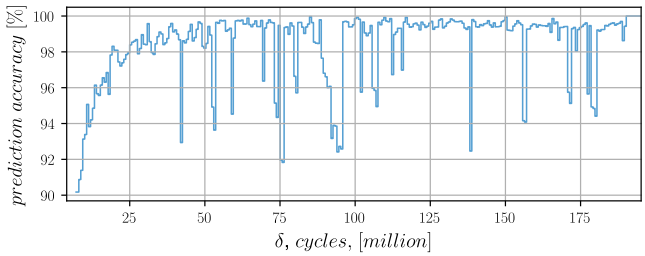

Fig. 12. Visualization of RUL model accuracy across cycles (δ) for the combined model, M.

temporal trend based on the established temporal reference model and extract α at $\delta = 0$. Given these values it is possible to establish a temporal α_δ for the joint en question.

D. Facilitating a Synthetic Dataset for Training

In light of the limited availability of real-world fault data, we employ the $F\sim$ distribution to generate a synthetic dataset for model training, enabling subsequent testing with the data that is authentic.

We extract the minimum and maximum α values from $F\sim$ across a normalized x-axis to define an occurrence area, A, within which 1500 data points are randomly generated. Because the number of protective stop log files for each joint is imbalanced, we do not prioritize regions. This set of data points is referred to as the $synthetic$ dataset and is shown in Fig. 10.

From $F\sim$ we compute a moving average and calculate the intersection with the temporal reference, ref, presented in Section V-A, to acquire an offset that allows locating the EoL of ref on the normalized axis, Δt. The offset is used to transform the normalized x-axis of $synthetic$ to program cycles, δ.

E. Training the Model, M

As established in Section IV, the correlation between the magnitude of stress imposed on the joint and the total operation time indicates that a dynamic α threshold is required for the model to scale. As depicted in Fig. 10, a range of different approximation functions are curve-fitted to describe the $synthetic$ dataset.

The model, denoted as M, is a sequence of approximation functions, $\mathbf{f}$. Each index in the sequence denotes a cycle, δ. With δ as input to M, the appropriate function can be extracted to calculate the expected EoL threshold, M_{EoL}. This is described in (9), where δ_i represents an index.

$$M_{EoL} = \mathbf{f}(\delta_i),\ \mathbf{f}(\delta_i) \mapsto M_{\{\delta_i\}} = \{\mathbf{f}_{\delta_0}(\delta_i), ..., \mathbf{f}_{\max(\delta)}(\delta_i)\} \tag{9}$$

As depicted in Fig. 11, to train the model, M, the cumulative distance of individual data points within the $synthetic$ dataset is computed relative to all approximation functions at every index. Subsequently, each index is mapped to the approximation function with the lowest summation of distances.

To estimate the EoL of the joint in question, the intersection point between M and the established α_δ is calculated. By isolating δ from (5) (refer to Section V-A), then given M_{EoL} as input, the calculation can be solved numerically according to (10).

$$(\delta_i == \delta_j)\,, \quad \delta_j = \frac{ln\left(\dfrac{M_{EoL} - \overline{x}_{[H(\alpha \leq \Omega(\alpha))]}}{\alpha_{[\delta=0]}}\right)}{\lambda} \tag{10}$$

where δ_j represents an index across the temporal α_δ sequence (from the robot joint) and δ_i an index in M such that $i = j$. The true EoL is found when δ_i is equal to δ_j.

In practice, this was implemented using binary search with an optimization threshold of 0.001. The RUL is finally computed by subtracting the current cycle count from δ_j. Note that Table I describes the overall training results on the left.

F. Testing and Validating the Model on Real Data

As previously established, the RUL model was trained on synthetic data. The validation of the model is conducted in two parts, using accuracy as the performance metric. The accuracy of each prediction was calculated using the absolute error, according to the description in (11). The same procedure was applied using the global maximum cycle count, $\delta_{\max} = 180$ cycles. Fig. 12 highlights the worst accuracies observed for each approximation function across the cycle indexes of M, based on training, testing and the case study.

$$wrt.groundtruth = 1 - \frac{|\delta_{groundtruth} - \delta_{prediction}|}{\delta_{groundtruth}} \tag{11}$$

Testing was conducted on the $F\sim$ distribution, and the results are seen in the center of Table I. This resulted in the overall worst-case accuracy of 90.3%. Furthermore, the most significant prediction error is -10.447 million program cycles. However, in this case, the prediction was 128.1, whereas the ground truth equaled 138.5 million cycles.

Validating the model was done based on a case study using two UR16e robots ($robot_0$ and $robot_1$). These were programmed to

TABLE I
HIGHLIGHTS THE RESULTS OBTAINED DURING TRAINING ON THE *Synthetic* DATASET AND TESTING ON THE $F \sim$ DISTRIBUTION AND THE ACCELERATED LIFE TEST ON TWO E-SERIES ROBOTS.

	training **dataset: synthetic**			*testing* **dataset: $F \sim$**			*validating* **dataset: robot 0 and 1**		
accuracy...	*max.*	*avg.*	*min.*	*max.*	*avg.*	*min.*	*max.*	*avg.*	*min.*
wrt. ground truth	100%	99.1%	90.2%	99.9%	96.1%	90.3%	99.1%	97.8%	96.6%
wrt. max δ	100%	99.8%	99.2%	99.9%	98.1%	94.6%	99.9%	99.8%	99.7%
cycles...	*min.*	*avg.*	*max.*	*min.*	*avg.*	*max.*	*min.*	*avg.*	*max.*
abs. error	0.0mil.	0.463mil.	1.591mil.	-0.074mil.	3.751mil.	-10.447mil.	-0.17mil.	0.338mil.	-0.506mil.

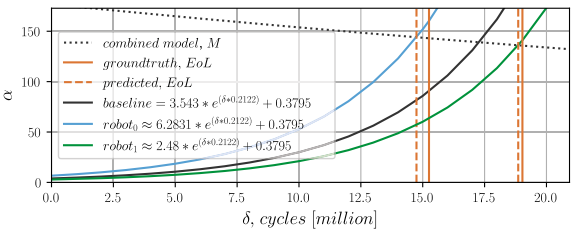

Fig. 13. Visualization of the EoL predictions of the two UR16e robots used in the accelerated life test case study.

execute identical sequences of instructions, encompassing high-speed repetitive horizontal and vertical swinging motions with no safety restrictions. Throughout the experiment, a program cycle counter was used to keep track of the number of repetitions. The experiment ran for 192 days. At the end, both robots had been worn beyond continuous operation. α was calculated with outset in the logs generated during the final protective stop, and temporal α_δ was computed based on the linear equation presented in Section V-C. The results are presented in the right side of Table I.

$robot_0$ operated for 15.2 million cycles. Our model predicted 14.7 with an error of -0.5 and an accuracy of 99.6%.

$robot_1$ operated for 19.02 million cycles. Our model predicted 18.8 with an error of -0.16 and an accuracy of 99.1%.

We emphasize that the robots used for training and testing the model differ from those employed in the case study (validation) phase. Additionally, it should be noted that external factors, such as temperature, have been variable throughout the case study. However, due to the duration of the study, the change in temperature and the consequent change in friction and wear have evened out. The results for $robot_0$ and $robot_1$ are visually depicted in Fig. 13.

Subsequent analysis revealed that in 72.4% of cases, our model predicts joints breaking down before actual ground truth.

G. Comparing the Results to a Baseline

In a preliminary investigation to select a comparative baseline, we employed diverse regression models including, among others, a MLP and a SVM to predict the RUL with estimated joint stress (α) as the input feature. However, the results exhibited suboptimal performance, with accuracies below 40% based on our current dataset. For that reason, we opted for the industry-standard equation for estimating the expected life of the gearbox (this was presented in (7)) [9], [10].

The calculation of $L10$ for $robot_0$ resulted in an expected lifetime of 9083 hours, while the actual life was 4224 hours. This prediction, therefore, exceeded the actual life by a factor of 2.1. Likewise, for $robot_1$, $L10$ was estimated at 7404 hours, whereas the actual life span was 4608 hours, yielding a deviation factor of 1.6.

Deviations with such magnitude can mislead an operator into expecting a significantly longer lifetime, rendering them ineffective for decision-making in maintenance processes. In comparison, our model estimates the joint life time significantly closer and ahead of actual ground truth, providing more certainty that the joint will last (or fail). Reliable information is crucial for efficient maintenance scheduling to potentially minimize unexpected downtime costs.

VI. DISCUSSION & FUTURE WORK

The potential of RUL predictions in robotics holds potential for enhancing reliability and maintenance decisions. Notably, the nature of our method implies that α is impacted by velocity, load, and environmental factors, enabling the potential to employ slow and cautious movements, thus avoiding the generation of significant JSFs and prolonging the robot's operation. This enables an additional design parameter that empowers developers to create programs optimized for prolonged operation.

Compared to existing research contributions, the holistic nature of our proposed method encompasses various components of the robot joint by taking outset in the robot control system, thereby facilitating predictions that consider a broader array of faults. However, the decision to zoom out only solves the challenge of root cause detection above the joint level. Therefore, further analysis is needed to identify and fully locate the type of fault.

There are several ways in which the RUL model can be finetuned. The first, of course, is to train it on a larger dataset. Nevertheless, the scarcity of fault data was a notable constraint in our testing phase and the case study, which spanned 192 days. When more data is available, further investigations using machine learning models may prove advantageous, warranting revisiting our comparative baseline analysis. Secondly, the model can be trained across several iterations rather than just one, and more approximation functions can be established to fit the input data. Finally, continuous approximations of the rate parameter, λ, could be employed, allowing temporal α_δ to align more closely with the true trend. Note that the results of our model directly correlate with the specific load case. Therefore, any alterations to the program necessitate rerunning the model to reflect the changing conditions accurately.

Though intuitively and theoretically possible, future research should prioritize evaluating the proposed model on collaborative robot joints not exclusive to UR robots, ensuring its applicability across a broader range of robotic systems. Perhaps our approach can also be transferred to other mechanical system domains, e.g., industrial robots.

VII. Conclusion

In conclusion, this letter introduces a holistic approach to estimating the stress experienced by a robot joint, denoted as α. This estimation considers various factors, including the robot's program, model, load, and environmental conditions.

Spanning the entire UR e-series, our experiments confirm that α serves as a real-time indicator of the joint's condition, with its magnitude increasing over time when subjected to stress. Moreover, α facilitates a knowledge-based prediction model for the RUL. This model is thoroughly evaluated in a case study and on a real-world dataset, demonstrating best-case prediction accuracies up to 99.9% and worst-case down to 90.3%. These results create the foundation for estimating the RUL of UR e-series robot joints to support decision-making in predictive maintenance.

References

[1] T. Nemeth, F. Ansari, W. Sihn, B. Haslhofer, and A. Schindler, "PriMa-X: A reference model for realizing prescriptive maintenance and assessing its maturity enhanced by machine learning," *Procedia CIRP*, vol. 72, pp. 1039–1044, 2018, doi: 10.1016/j.procir.2018.03.280.

[2] B. Schmidt, L. Wang, and D. Galar, "Semantic framework for predictive maintenance in a cloud environment," *Procedia CIRP*, vol. 62, pp. 583–588, 2017, doi: 10.1016/j.procir.2016.06.047.

[3] T. Zonta, C. A. da Costa, R. da Rosa Righi, M. J. Lima, E. S. da Trindade, and G. P. Li, "Predictive maintenance in the industry 4.0: A systematic literature review," *Comput. Ind. Eng.*, vol. 150, 2020, Art. no. 106889, doi: 10.1016/j.cie.2020.106889.

[4] J. Lee, J. Ni, D. Djurdjanovic, H. Qiu, and H. Liao, "Intelligent prognostics tools and e-maintenance," *Comput. Ind.*, vol. 57, no. 6, pp. 476–489, 2006, doi: 10.1016/j.compind.2006.02.014.

[5] L. Ren, Y. Sun, J. Cui, and L. Zhang, "Bearing remaining useful life prediction based on deep autoencoder and deep neural networks," *J. Manuf. Syst.*, vol. 48, pp. 71–77, 2018, doi: 10.1016/j.jmsy.2018.04.008.

[6] M. Xia, T. Li, L. Liu, L. Xu, and C.W. de Silva, "Intelligent fault diagnosis approach with unsupervised feature learning by stacked denoising autoencoder," *Inst. Eng. Technol.*, vol. 11, no. 6, pp. 687–695, 2017, doi: 10.1049/iet-smt.2016.0423.

[7] M. He and D. He, "Deep learning based approach for bearing fault diagnosis," *IEEE Trans. Ind. Appl.*, vol. 53, no. 3, pp. 3057–3065, May/Jun. 2017, doi: 10.1109/TIA.2017.2661250.

[8] X. Li, H. Shao, G. Li, W. Liu, and C. Liu, "Static simulation and structure optimization of key parts of joint welding robots," in *Proc. IEEE Int. Conf. Mechatronics Automat.*, 2018, pp. 282–287, doi: 10.1109/ICMA.2018.8484469.

[9] Harmonic Drive Group, Engineering Data, "SHG-2UH / 2S0 / 2SH Units," Dec. 2018. Accessed: Oct. 22, 2023. [Online]. Available: https://harmonicdrive.de/fileadmin/user_upload/ED_SHG_2UH_2SO_2SH_E_1021387_12_2018_V02.pdf

[10] Harmonic Drive LLC, "Cup type component sets & housed units," 800-921-3332, 2016. Accessed: Oct. 22, 2023. [Online]. Available: https://www.harmonicdrive.net/_hd/content/documents/csf-csg.pdf

[11] J. Man and Q. Zhou, "Prediction of hard failures with stochastic degradation signals using wiener process and proportional hazards model," *Comput. Ind. Eng.*, vol. 125, pp. 480–489, 2018, doi: 10.1016/j.cie.2018.09.015.

[12] Q. Zhou, J. Son, S. Zhou, X. Mao, and M. Salman, "Remaining useful life prediction of individual units subject to hard failure," *IIE Trans.*, vol. 46, no. 10, pp. 1017–1030, 2014, doi: 10.1080/0740817X.2013.876126.

[13] J. Yan, Y. Meng, L. Lu, and L. Li, "Industrial Big Data in an industry 4.0 environment: Challenges, schemes, and applications for predictive maintenance," *IEEE Access*, vol. 5, pp. 23484–23491, 2017, doi: 10.1109/ACCESS.2017.2765544.

[14] M. Saez, F. Maturana, K. Barton, and D. Tilbury, "Anomaly detection and productivity analysis for cyber-physical systems in manufacturing," in *Proc. 13th IEEE Conf. Automat. Sci. Eng.*, 2017, pp. 23–29, doi: 10.1109/COASE.2017.8256070.

[15] W. Dazhong, J. Connor, T. Janis, G. Robert, and K. Soundar, "Data-driven prognostics using random forests: Prediction of tool wear," *Int. Manuf. Sci. Eng. Conf.*, vol. 3, 2017, Art. no. V003T04A048, doi: 10.1115/MSEC2017-2679.

[16] C. Nentwich and G. Reinhart, "Towards data acquisition for predictive maintenance of industrial robots," *Procedia CIRP*, vol. 104, pp. 62–67, 2021, doi: 10.1016/j.procir.2021.11.011.

[17] M. Saeed et al., "Spline-based trajectory generation to estimate execution time in a robotic assembly cell," *Int. J. Adv. Manuf. Technol.*, vol. 121, pp. 6921–6935, 2022, doi: 10.1007/s00170-022-09792-y.

[18] E. S. Kolvig-Raun, M. B. Kjærgaard, and R. Brorsen, "EDDE: An event-driven data exchange to accurately introspect cobot applications," in *Proc. IEEE/ACM 5th Int. Workshop Robot. Softw. Eng.*, 2023, pp. 25–30, doi: 10.1109/RoSE59155.2023.00009.

[19] S. Nie, Y. Li, G. Shuai, S. Tao, and F. Xi, "Modeling and simulation for fatigue life analysis of robots with flexible joints under percussive impact forces," in *Proc. Robot. Comput.-Integr. Manuf.*, 2016, pp. 292–301, doi: 10.1016/j.rcim.2015.04.001.

[20] E. Madsen, O. S. Rosenlund, D. Brandt, and X. Zhang, "Comprehensive modeling and identification of nonlinear joint dynamics for collaborative industrial robot manipulators," *Control Eng. Pract.*, vol. 101, 2020, Art. no. 104462, doi: 10.1016/j.conengprac.2020.104462.

[21] J. Heredia, C. Schlette, and M. B. Kjærgaard, "Data-driven energy estimation of individual instructions in user-defined robot programs for collaborative robots," *IEEE Robot. Automat. Lett.*, vol. 6, no. 4, pp. 6836–6843, Oct. 2021, doi: 10.1109/LRA.2021.3094781.

[22] P. C. Krause, O. Wasynczuk, S. D. Sudhoff, and S. Pekarek, *Analysis of Electric Machinery and Drive Systems*. Hoboken, NJ, USA: Wiley, 2013.

[23] Universal Robots Support, "Real-time data exchange (RTDE) guide," Oct. 10, 2019. Accessed: Oct. 22, 2023. [Online]. Available: https://www.universal-robots.com/articles/ur/interface-communication/real-time-data-exchange-rtde-guide/

[24] T. Borgi, A. Hidri, B. Neef, and M. S. Naceur, "Data analytics for predictive maintenance of industrial robots," in *Proc. Int. Conf. Adv. Syst. Electric Technol.*, Hammamet, Tunisia, 2017, pp. 412–417, doi: 10.1109/ASET.2017.7983729.

[25] L. Pust, F. Peterka, G. Stépán, G. R. Tomlinson, and A. Tondl, "Nonlinear oscillations in machines and mechanisms theory, mechanism and machine theory," *Mechanism Mach. Theory*, vol. 34, no. 8, pp. 1237–1253, 1999, doi: 10.1016/S0094-114X(98)00068-8.